Geophysical Research Letters

RESEARCH LETTER
10.1029/2023GL105554

Zonal Structure of Tropical Pacific Surface Salinity Anomalies Affects the Eastern and Central Pacific El Niños Differently

Cong Guan[1,2], Feng Tian[1,2], Michael J. McPhaden[3], Shijian Hu[1,2], and Fan Wang[1,2]

[1]Key Laboratory of Ocean Circulation and Waves, Institute of Oceanology, Chinese Academy of Sciences, Qingdao, China, [2]Laoshan Laboratory, Qingdao, China, [3]NOAA/Pacific Marine Environmental Laboratory, Seattle, WA, USA

Key Points:

- Salinity anomalies in the central Pacific induce the strongest surface warming during both types of El Niño, tapering off to the east and west
- The distinct sea surface salinity zonal structures between the two El Niños amplify their difference in sea surface temperature magnitude by about 10%
- Salinity effects on vertical mixing and entrainment account for the different eastern Pacific and central Pacific El Niño responses

Supporting Information:

Supporting Information may be found in the online version of this article.

Correspondence to:

F. Wang,
fwang@qdio.ac.cn

Citation:

Guan, C., Tian, F., McPhaden, M. J., Hu, S., & Wang, F. (2023). Zonal structure of tropical Pacific surface salinity anomalies affects the eastern and central Pacific El Niños differently. *Geophysical Research Letters*, *50*, e2023GL105554. https://doi.org/10.1029/2023GL105554

Received 18 JUL 2023
Accepted 13 OCT 2023

Abstract Maximum sea surface salinity (SSS) anomalies are found in the central Pacific during the eastern Pacific El Niño (EPEN) and located further westward during the central Pacific El Niño (CPEN), but whether these differences affect event strengths is unclear. By performing ocean general circulation model experiments via modifying freshwater flux anomalies, we find salinity effects on surface warming during both types are highly sensitive to zonal locations of SSS anomalies, with the strongest warming induced by the SSS anomalies near the international dateline. Further analysis reveals that vertical mixing and entrainment dominate this temperature sensitivity, with the strongest response to SSS anomalies occurring in the central Pacific. The central-Pacific SSS anomalies increase EPEN warming by 0.15°C while the westward-located SSS anomalies make little contribution to CPEN warming. Therefore, the distinct zonal structures of SSS anomalies facilitate stronger EPEN than the CPEN, increasing their difference in intensity by about 10%.

Plain Language Summary The El Niño-Southern Oscillation (ENSO) is the strongest year-to-year climate variability in the planet. The central Pacific El Niño (CPEN) have been recognized in recent decades, with weaker surface warming located more westward, in contrast to the traditional eastern Pacific El Niño (EPEN). Previous studies have underscored various air-sea processes in shaping these differences, however, the impact of salinity remains unknown. Here based on ocean model experiments, we found the salinity effect on El Niño warming is very sensitive to zonal locations of salinity anomalies. The salinity anomalies located in the central Pacific are more effective in modulating local ocean vertical stratification, weakening the colder subsurface water into the mixed layer and further enhancing the surface warming. Therefore, the central equatorial Pacific-located salinity anomalies during EPEN contributes to its stronger warming than those west-located salinity anomalies during CPEN, enhancing the sea surface temperature difference between the two events by about 10%. Our results provide new insight in understanding the ENSO diversity and also its low-frequency variability, which may be helpful for interpreting more complex model simulations and for and predicting ENSO variations.

1. Introduction

The El Niño-Southern Oscillation (ENSO) has significant impacts on global climate (McPhaden et al., 2006). Its warm phase El Niño, occurs conventionally with positive sea surface temperature (SST) anomalies generated in the eastern equatorial Pacific. A new type of El Niño is detected and occurs more frequently in recent decades with the largest SST anomalies in the central Pacific (Lee & McPhaden, 2010), known as dateline El Niño (Larkin and Harrison, 2005a, 2005b), El Niño Modoki (Ashok et al., 2007), central Pacific El Niño (Kao & Yu, 2009), or warm pool El Niño (Kug et al., 2009). Here we refer to these two types as EP El Niño (EPEN) and CP El Niño (CPEN). Understanding this diversity is one of the essential ways to understand ENSO complexity under climate change (Cai et al., 2020; Geng et al., 2022; Timmermann et al., 2018).

Sustained attention has been paid to their differences and associated mechanisms in terms of atmospheric-oceanic dynamics (e.g., Guan & McPhaden, 2016; Kug et al., 2009; Ren & Jin, 2013). As an important factor that determines the sea surface density, sea surface salinity (SSS) is found to have large negative anomalies in the tropical Pacific during El Niño events (e.g., Schneider, 2004). These salinity anomalies modify the vertical ocean stratification and lead to a thicker barrier layer between the mixed layer and isothermal layer. It weakens the vertical entrainment of subsurface cold water and vertical mixing at the bottom of the mixed layer, and hence warms the upper layer, further exerting a positive feedback (Ando & McPhaden, 1997; Maes et al., 2002, 2006; Bosc et al., 2009; Vialard & Delecluse, 1998a, 1998b; Vialard et al., 2002; Zhang et al., 2012). Model studies showed

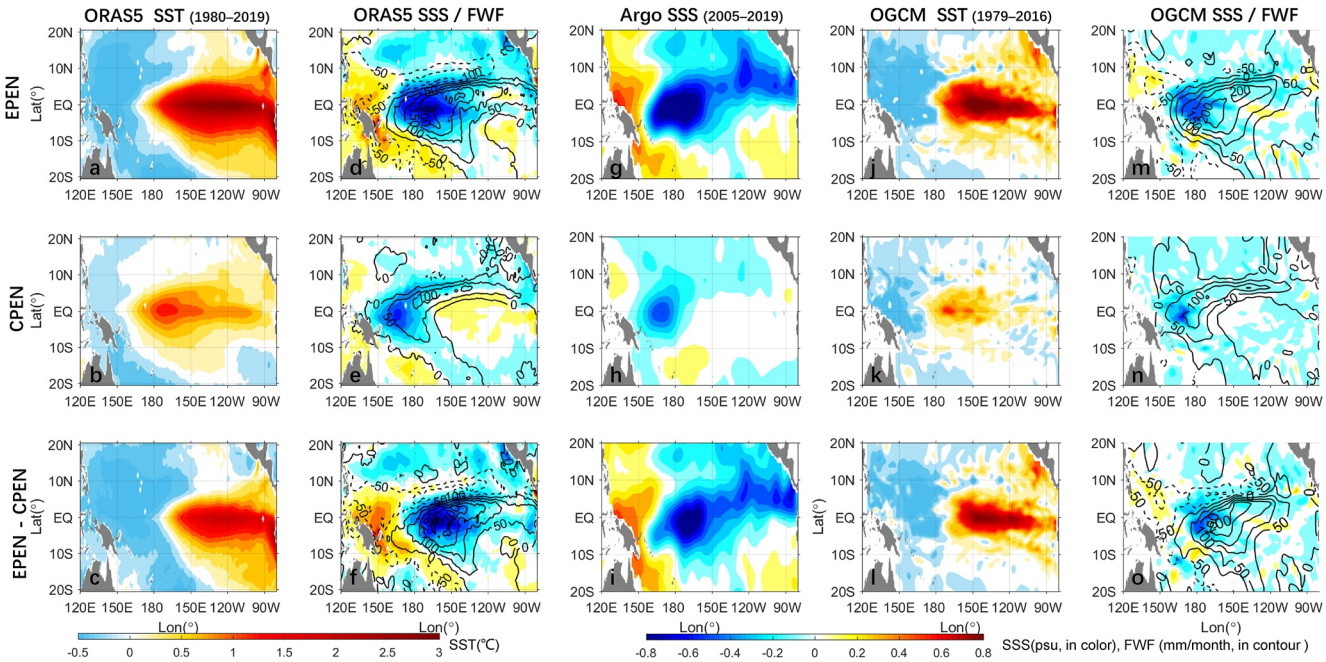

Figure 1. Anomalies of SST, SSS and FWF during the mature phase of EPEN (upper) and CPEN (middle) and their differences (bottom), respectively based on ORAS5 reanalysis, Argo observation, and OGCM simulation.

that improving the representation of salinity effects helps better simulate ENSO variability in ocean general circulation and coupled models (e.g., Maes et al., 2005; Zhang, 2015; Zhao et al., 2014).

Previous studies found tropical Pacific salinity anomalies show distinct characteristics in terms of zonal pattern and time evolution between EPEN and CPEN (e.g., Singh et al., 2011). Qi et al. (2019) found that salinity anomalies are in the tropical central Pacific during EPEN, which are located more eastward by 25° on longitude than those in the western Pacific during CPEN. Zhi et al. (2020, 2021) pointed out that the salinity anomalies in EPEN lead the Niño index by 8–10 months but there is no apparent lead-lag relation between the salinity and CPEN, implying different salinity roles in these two types. As shown in Zheng et al. (2014), salinity anomalies in the central Pacific have larger effects on modifying the upper-layer vertical stratification than those in the western Pacific. Guan et al. (2022) further examined SSS zonal patterns in affecting ENSO asymmetry in an ocean model, and found that central-Pacific SSS anomalies have larger impacts on ENSO development. Therefore, the questions arise: will the zonal patterns of salinity anomalies affect EPEN and CPEN differently; and if so, what are the underlying dynamical processes? In this study, we will address these questions by executing ocean general circulation model (OGCM) sensitivity experiments.

In the rest of this paper, we will describe data and experimental design in Section 2, followed by an investigation of the sensitivity of EPEN and CPEN to SSS anomaly longitude in Section 3. The salinity effects on the EPEN and CPEN SST anomalies are then examined in Section 4 and we will summarize the results and discuss remaining issues in Section 5.

2. Data and Model Design

The OGCM used in this study is a primitive equation and reduced gravity model with a vertical sigma (σ) coordinate (Gent & Cane, 1989). It covers the tropical Pacific basin and has 20 layers vertically with a mixed layer as the surface layer determined by a mixed layer model (Chen et al., 1994). These data are monthly over 1979–2016. In this model, freshwater flux (FWF) forcing can directly change the surface salinity and affect the entire upper-ocean thermal-dynamics (e.g., Gao et al., 2020). The OGCM is well suited for simulating dynamical variabilities in the equatorial Pacific including thermohaline characteristic and mixed layer dynamics (Figure 1 and Figure S1 in Supporting Information S1), and has been widely used to investigate the effects of FWF and surface salinity on ENSO (e.g., Guan et al., 2022; Luo et al., 2005; Murtugudde & Busalacchi, 1998; Zhang & Busalacchi, 2009; Zhang et al., 2018).

We also use gridded Argo data over 2005–2019 and the ECMWF Ocean Reanalysis System 5 (ORAS5) over 1980–2019 for the comparisons of temperature and salinity patterns during EPEN and CPEN with the OGCM. They are both monthly with a horizontal resolution of 1° × 1°. EPENs/CPENs are selected referring to the consensus events (EPEN: 1982–1983, 1986–1987, 1997–1998, 2015–2016; CEPN: 1987–1988, 1994–1995, 2002–2003, 2004–2005, 2006–2007, 2009–2010, 2014–2015) in Capotondi et al. (2020) and additionally the 1991–1992 EPEN and 2018–2019 CPEN (Guan et al., 2023; Sullivan et al., 2016). Events for composite are selected in respective time span for Argo, ORAS5 and OGCM (see detailed in Table S1 in Supporting Information S1).

OGCM experiments are also executed in 2-year composite EPEN and CPEN based on events during 1979–2016. The control experiment is set by forcing the ocean model by corresponding El Niño composites of wind stress and climatological FWF. We determine salinity patterns by tuning the FWF interannual anomalies to perform a series of sensitivity experiments. This method can well represent the intensity of interannual SSS anomalies in the spatial pattern. We afterward refer to FWF effects as salinity effects. More details on the model and experimental designs are shown in the next two sections and also the Table S2 in Supporting Information S1.

3. Different Zonal Structures of Salinity Anomalies in EPEN and CPEN

Figure 1 shows the interannual anomalies of SST, SSS, and FWF during mature phases of EPEN and CPEN. Based on ORAS5, the EPEN warming is located more eastward and has a larger amplitude than those during CPEN, with their difference depicted as stronger positive SST skewness to the east of the dateline, consistent with previous studies (e.g., Guan, McPhaden, et al., 2019; Kug et al., 2009). During EPEN, prominent positive FWF anomalies and its associated negative SSS anomalies are found in the central equatorial Pacific (CEP), in contrast to those west-located anomalies during CPEN. Take the isohaline of −0.4 psu for example, the EPEN SSS anomalies reach 150°W at equator, 40° in longitude more eastward than CPEN. Argo observation reveals similar anomalous SSS patterns but much larger up to 0.8 psu during EPEN, probably attributed to different time spans for the composite. The difference between the two types presents as an SSS zonal dipole, similar to the salinity dipole in response to El Niño-La Niña asymmetry (Guan, Hu, et al., 2019; Guan et al., 2022). The OGCM captures the SST structures well for both types (Figures 1j–1o). Under the surface wind stress and FWF forcing, SSS anomalies are similar to those in Argo and ORAS5, albeit with smaller amplitudes for both events.

SSS and SST anomalies in response to interannual FWF anomalies for both events are shown in Figure 2. Maximum positive FWF and negative SSS anomalies during EPEN are very strong (up to 180 mm month^{-1} for the FWF and 0.2 psu for the SSS), located at around 160°W in the CEP and propagate eastward. As for CPEN, maximum FWF and SSS anomalies are much weaker and located west to 170°E. The CEP gets clearly warmer during both events, especially with maxima in the Niño 4 region (5°N–5°S, 160°E–150°W) in their mature phases. The salinity-effect warming during EPEN is much stronger up to 0.2°C and extends to the eastern Pacific, while the CPEN warming is weaker and limited around the dateline. As differences between the two events, FWF presents contrasting anomalous trends: freshening and warming east of the dateline in contrast with salinification and cooling to the west (Figures 2f and 2i). We note that these salinity-effect SST difference are consistent with the total SST difference as in Figure 1, indicating that zonal structures of FWF and salinity can reinforce the differences between EPEN and CPEN SST.

4. The Sensitivity of EPEN and CPEN SST to SSS Anomaly Longitude

We first diagnosed whether El Niño SST are sensitive to SSS anomaly longitude during both events. A FWF window is set with positive anomalies spanning 40° zonally on the equator (Figure 3a). The magnitude is spatially uniform, but temporally varies from 60 mm/month in July, increases gradually to the mature phase, and then decays to June the next year. The anomalous evolution is set with reference to Figures 2a and 2b, but with double amplitudes in order to construct SSS anomalies that are close to the observations during El Niño as in Figure 1 (Guan et al., 2022). We slide the FWF window with its central longitude moving from 140°E to 120°W, to conduct 11 sensitivity experiments during either event (Figures S2 and S3 in Supporting Information S1). Considering the induced SST anomalies are basically in the central Pacific (Figure 2), we use the mature phase SST anomaly averaged in the Niño4 region to indicate salinity effects in each experiment, marked as each black circle in Figures 3b and 3c.

Results show that SST anomalies during both events are highly sensitive to different SSS zonal locations among the experiments. When the FWF window is set in the CEP, the induced SST anomalies exceed 0.1°C. More

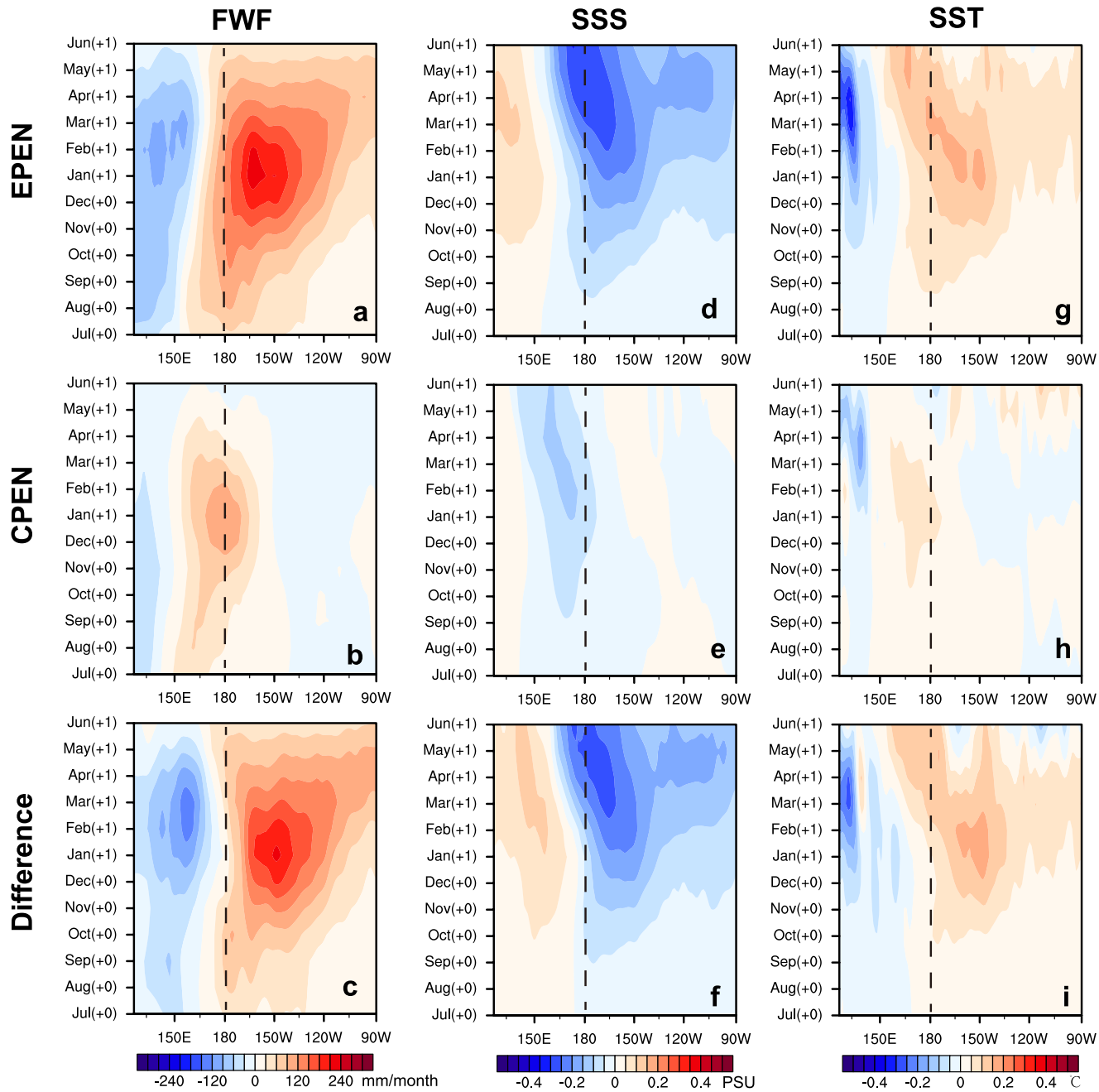

Figure 2. Composite FWF anomalies (left) and their forced SSS (middle) and SST (right) anomalies in the equatorial Pacific during the two types of El Niños and their differences.

specifically from 180° to 170°W, SST anomalies are the strongest as up to 0.13°C for both events. And these effects on SST are gradually decreased to the SSS zonal locations in the east and west. Therefore, FWF and salinity effects on El Niño SST are the largest when the anomalies occur in the CEP for both El Niños.

To further examine the specific oceanic processes that control this warming sensitivity to different SSS zonal locations, we diagnosed heat budgets in the mixed-layer Niño4 region during the developing phases (defined as August [0]-November [0]) for either event. The equation is expressed as, $\frac{\partial T}{\partial t} = -u\frac{\partial T}{\partial x} - v\frac{\partial T}{\partial y} - w\frac{\partial T}{\partial z} + Q_{ent+mix} + Q_{net}$, where the left side is the temperature tendency and the right-side terms are zonal advection, meridional advection, vertical advection, vertical mixing and entrainment at the base of the mixed layer, and net sea surface heat flux, respectively. In Figures 3b and 3c, temperature tendencies are all positive. Vertical mixing and entrainment

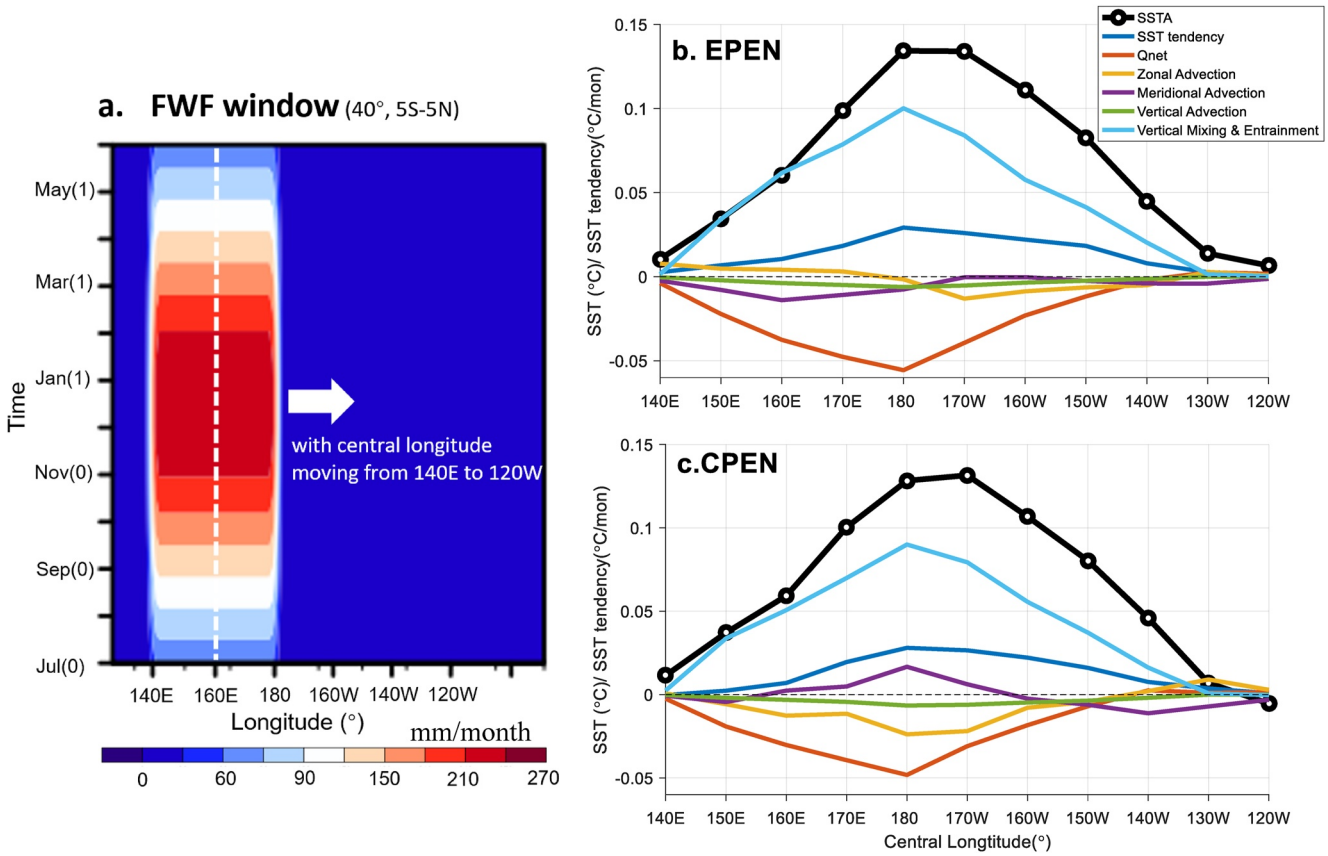

Figure 3. The FWF sliding window (a) and its forced anomalies of SST (thick black lines) during the mature phases and temperature budget terms (color lines) during the developing phases of EPEN (b) and CPEN(c) averaged in the Niño4 region. The X-coordinates of (b) and (c) are the central longitudes of the FWF forcing window.

is the largest positive term and reaches its strongest up to 0.1°C/month, when the FWF window is centered at 180° during both events. Its warming effect is partly damped by the negative sea surface net heat flux, which also peaks at about −0.05°C/month when the window is set near the dateline. During CPEN, meridional advection is slightly positive up to 0.02°C/month and zonal advection is negative with its strongest magnitude of −0.02°C/month in the central-Pacific experiments. Other terms are relatively weaker. Therefore, the warming sensitivity to SSS locations is attributed to the vertical mixing and entrainment, which is more effective in the CEP.

5. Salinity Effects on the EPEN and CPEN SST Anomalies

In this section, we designed two FWF scenarios more specifically based on the FWF anomalies during EPEN and CPEN for sensitivity experiments (Figures 2a and 2b). Since the magnitude of EPEN FWF anomalies is larger than that during CPEN, we normalized these two scenarios as, $\mathrm{FWF_{WEP}} = \alpha \times \frac{A_{CPEN}+A_{EPEN}}{2A_{CPEN}} \times \mathrm{FWF}_{CPEN}$, $\mathrm{FWF_{CEP}} = \alpha \times \frac{A_{CPEN}+A_{EPEN}}{2A_{EPEN}} \times \mathrm{FWF}_{EPEN}$, where $\alpha = 2$ is twice the FWF anomalies in Figure 2, and A is the amplitude of composite El Niño based on the Niño 3.4 index during 1979–2016 ($A_{CPEN} = 1.01$°C, $A_{EPEN} = 1.97$°C). Therefore, we obtain 2.97 times the FWF anomalies during CPEN and 1.51 times the FWF anomalies during EPEN to carry out two groups of sensitivity experiments in either El Niño event. As in Figure 4, these two FWF cases have similar amplitudes but different zonal structures, with their differences as clearly contrastive evolutions on either side of the dateline. Considering the distinct maximum FWF anomalies located in the western equatorial Pacific (WEP) and CEP receptivity, we refer them to the WEP case and CEP case, respectively.

Forced by these two FWF cases, salinity anomalies present different zonal structures: the CEP-case salinity anomalies are located more eastward by generally 15° and have larger zonal distribution extending to the eastern Pacific compared to those in the WEP case during both events. The SSS differences between the two cases show dipole structures with the dateline as the axis, which is appropriate for the comparison experiments. In response

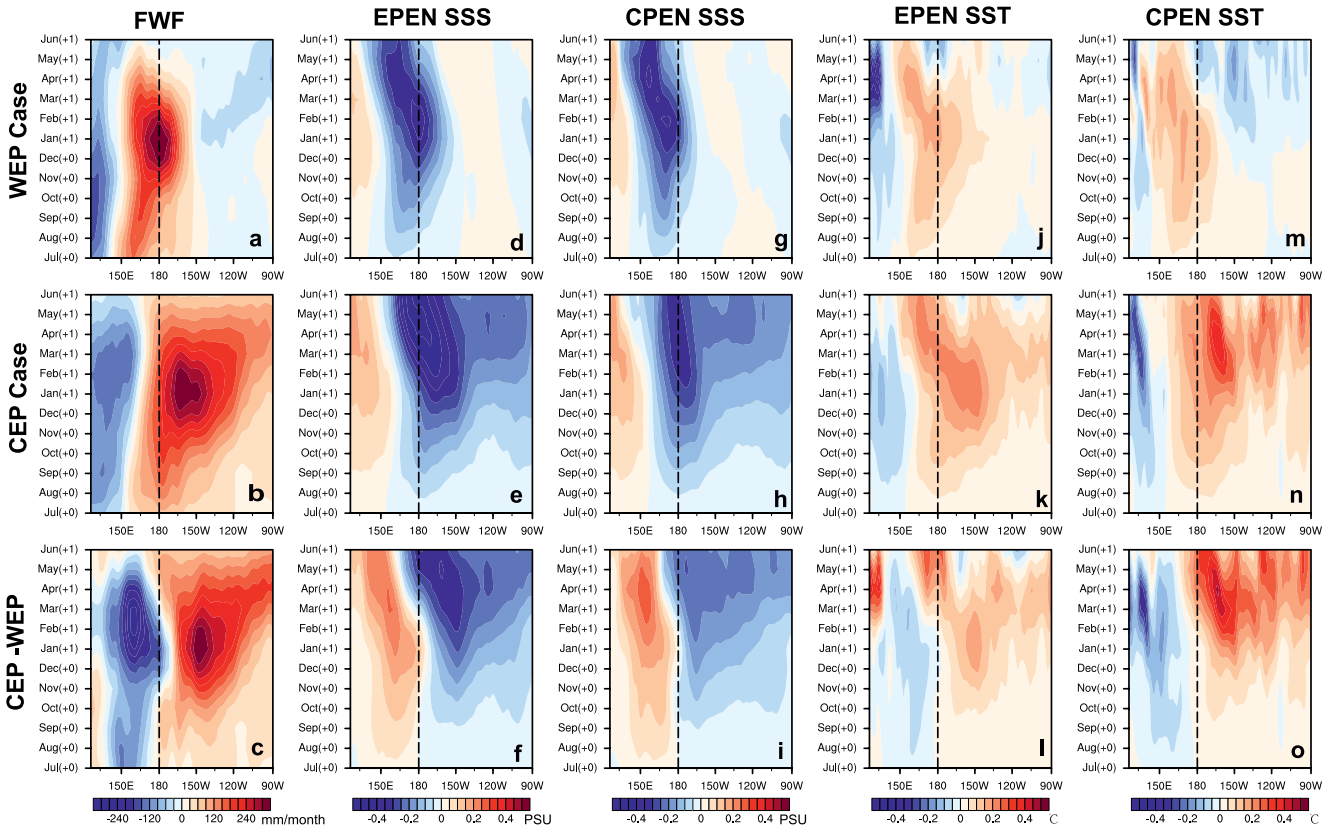

Figure 4. The WEP and CEP cases of FWF anomalies (a–c) and its forced anomalies of SSS (d–i) and SST (j–o) during the EPEN and CPEN on the equator.

to these salinity effects, there are obviously anomalous warming in the equatorial central-eastern Pacific for all the experiments (Figures 4j, 4k, 4m, and 4n). For the WEP case, positive SST anomalies during both events are generated along the 165°E and extend gradually to the east but still with its maximum (exceeding 0.1°C) concentration west of the dateline in the mature phase (Figures 4j and 4m). For the CEP case, the anomalous warming propagates clearly to the eastern Pacific, and has a larger amplitude up to 0.2°C at around 150°W in both the mature phases (Figures 4k and 4n).

During El Niño mature phases, the CEP-case salinity induce clearly larger warming east of the dateline compared to the WEP case (Figures 5a and 5b). Heat budgets are also analyzed in both cases to access different roles of underlying air-sea processes (Figures 5c and 5d). During EPEN, SST tendencies are all positive dominated by the vertical entrainment and mixing at the base of the mixed layer. Net surface heat flux is the largest negative term and the ocean advections are relatively weak. Compared to the WEP cases, the stronger positive vertical mixing and entrainment dominants the stronger warming in the CEP cases during both events, followed by the weaker negative net surface heat flux during EPEN and stronger negative zonal advection during CPEN.

Salinity effects on Niño indices for the two cases are shown in Figures 5e and 5f. Black lines and shading bars depict the SST amplitudes induced by only the wind simulated in the OGCM. The CEP case leads to extra EPEN warming in Niño 4 by 0.13°C and in Niño3.4 by 0.15°C, enhancing the warming by 25% in Niño4 and 8% in Niño 3.4. During CPEN, the CEP-case FWF increases the Niño4 warming by 0.14°C (38%) and Niño3.4 by 0.10°C (20%). However, these warming effects in the WEP case are found only noteworthy in Niño4, increasing the EPEN warming by 0.10°C (18%) and CPEN warming by 0.09°C (25%).

Considering that the zonal patterns of FWF and salinity anomalies are observed different as the WEP case during CPEN and the CEP case during EPEN, how much does the difference in SSS zonal structure contribute to the amplitude difference of the two El Niños? Take the Niño3.4 index for example, the wind-forced amplitude difference between EPEN and CPEN is 1.26°C in this OGCM. Assuming these two events are forced by the same FWF case, the amplitude difference is only 1.30°C for the WEP case and 1.31°C for the CEP case, which increases

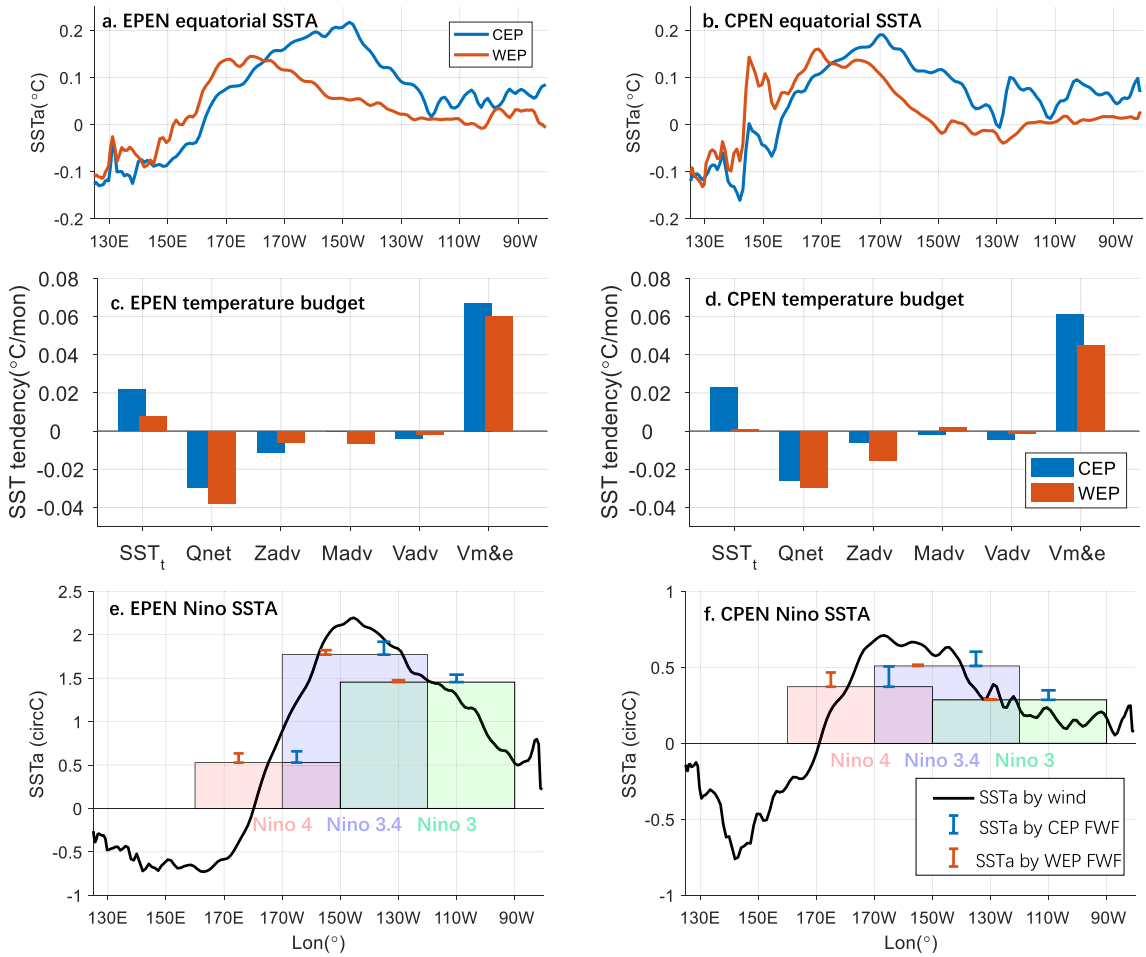

Figure 5. SST anomalies forced by the CEP and WEP FWF cases in the equatorial Pacific (5°S–5°N) during the mature phases of EPEN (a) and CPEN (b). Temperature budget terms averaged in the Niño4 region during the developing phases are shown in (c) and (d). Salinity warming effects on Niño indices are shown as error bars in (e) and (f), in comparison with the wind-forced El Niño warming (shown in black line and shading bars).

the wind-forced difference by 3% and 4% respectively. However, when these are the CEP case during EPEN and WEP case during CPEN, the difference is 1.40°C, which increases the wind-forced SST difference by 11%. Therefore, the different zonal structures of SSS anomalies clearly reinforce the stronger EPEN than the CPEN, via the vertical entrainment and mixing.

6. Summary and Discussion

It is well known that the SST anomalies occur more eastward and have larger amplitude during the eastern Pacific El Nino (EPEN) than those during the central Pacific El Niño (CPEN). In response to the two types of El Niño, stronger SSS anomalies are located in the CEP during EPEN, while those during CPEN are located more westward (referred to the WEP). Considering potential stronger salinity effects in the CEP on El Niño warming, this study examined how these different zonal structures of SSS affect the two types of El Nino based on OGCM experiments.

We find that during both events positive SST anomalies induced by salinity effects are highly sensitive to the zonal locations of FWF and have the largest amplitude when the FWF and salinity anomalies occur in the CEP in between 180° and 170°W. Temperature budget analysis revealed that this sensitivity is dominated by the vertical mixing and entrainment process.

To further diagnose how the different SSS zonal structures affect the two types of El Niño, WEP-case and CEP-case FWF experiments are applied alternatively to either event to execute sensitivity experiments. Results

show that during both events the CEP-case salinity can induce larger El Nino warming that extends more eastward than those in the WEP case. The CEP-case salinity effects during EPEN and the WEP case during CPEN enhance the intensity difference between the two El Niño by 11%, compared to the difference under the same case by 3%–4%. Therefore, the different zonal structures of SSS anomalies clearly facilitate stronger EPEN than the CPEN, enlarging their difference in intensity.

Our results emphasize salinity's role in affecting El Niño diversity. During El Niño, negative SSS anomalies in the western-central equatorial Pacific enhances vertical stratification as with a shallower mixed layer and weakened vertical temperature gradient under the mixed layer, which suppresses the entrainment of colder subsurface waters into the mixed layer and also weakens the vertical mixing (Figure S4 in Supporting Information S1). These processes can be explicitly simulated included in the vertical entrainment and mixing term in this OGCM. Consistent with Guan et al. (2022), we found that the CEP is a unique region to facilitate the salinity effects on the development of ENSO events. Zheng et al. (2014) pointed out that salinity dominates the interannual variability of CEP upper-layer stratification. Here we confirm that salinity affects SST in the CEP primarily through the strongest vertical entrainment and mixing there. Why salinity has such a large effect in the CEP can be attributed to the background conditions in the tropical Pacific. During an El Niño when the trade wind weakens and the equatorial thermocline gets less tilted, the CEP acts like the fulcrum of a zonal seesaw. The vertical temperature structure does not change much here compared to the significant changes to the west and east, but it is where the maximum salinity anomalies are found along the equator with its maximum at the surface. These variations in the CEP lead to clearly shoaling of the mixed layer but little change in the isothermal layer, which then weakens the entrainment of colder subsurface water into the mixed layer and further enhances the surface warming. We also note that some model biases (such as caused by vertical coordinate structures) may exist since we examined these processes in only one model, and also that salinity effects on ENSO SST may be underestimated because of neglected positive air-sea coupling processes (Gao et al., 2020). The results of this study nonetheless provide additional insights into ENSO diversity and may help guide improvements our ability to simulate and predict ENSO variations.

Data Availability Statement

The Argo data, ECMWF ORAS5 (Zuo et al., 2017), NOAA/OAR/ESRL PSD SST (Huang et al., 2017), NCEP/NCAR wind stress reanalysis (Kalnay et al., 1996), GPCP precipitation (Adler et al., 2003) and OAflux evaporation (Yu & Weller, 2007) used are available online at the IPRC Asian Pacific Data Research Center. Niño indices are from NOAA climate prediction center. OGCM Data is available at Feng (2023).

Acknowledgments
The authors thank the two anonymous reviewers for their constructive comments on the original version of this manuscript. This work was supported by the National Natural Science Foundation of China (Grants 42176008) and the Youth Innovation Promotion Association of CAS (2023214). F. Wang is supported by the he NSFC Innovative Group Grant (No. 42221005) and National Key R&D program (2022YFF0801401). PMEL contribution no. 5541.

References

Adler, R. F., Huffman, G. J., Chang, A., Ferraro, R., Xie, P.-P., Janowiak, J., et al. (2003). The version-2 global precipitation climatology project (GPCP) monthly precipitation analysis (1979-present) [Dataset]. Journal of Hydrometeorology, *4*(6), 1147–1167. https://doi.org/10.1175/1525-7541(2003)004<1147:TVGPCP>2.0.CO;2

Ando, K., & McPhaden, M. J. (1997). Variability of surface layer hydrography in the tropical Pacific Ocean. *Journal of Geophysical Research*, *102*(C10), 23063–23078. https://doi.org/10.1029/97jc01443

Ashok, K., Behera, S. K., Rao, S. A., Weng, H., & Yamagata, T. (2007). El Niño Modoki and its possible teleconnection. *Journal of Geophysical Research*, *112*(C11), C11007. https://doi.org/10.1029/2006jc003798

Bosc, C., Delcroix, T., & Maes, C. (2009). Barrier layer variability in the western Pacific warm pool from 2000 to 2007. *Journal of Geophysical Research*, *114*(C6), C06023. https://doi.org/10.1029/2008jc005187

Cai, W., Ng, B., Geng, T., Wu, L., Santoso, A., & McPhaden, M. J. (2020). Butterfly effect and a self-modulating El Niño response to global warming. *Nature*, *585*(7823), 68–73. https://doi.org/10.1038/s41586-020-2641-x

Capotondi, A., Wittenberg, A. T., Kug, J.-S., Takahashi, K., & McPhaden, M. (2020). ENSO diversity. In A. Santoso, W. Cai, & M. McPhaden (Eds.), *El Niño Southern Oscillation in a changing climate* (pp. 65–86). American Geophysical Union (AGU). https://doi.org/10.1002/9781119548164.ch4

Chen, D., Rothstein, L. M., & Busalacchi, A. J. (1994). A hybrid vertical mixing scheme and its application to tropical ocean models. *Journal of Physical Oceanography*, *24*(10), 2156–2179. https://doi.org/10.1175/1520-0485(1994)024<2156:ahvmsa>2.0.co;2

Feng, T. (2023). Model data for Guan et al., 2023 "Zonal structure of tropical Pacific surface salinity anomalies affects the eastern Pacific El Nino and central Pacific El Nino [Dataset]. Figshare. https://doi.org/10.6084/m9.figshare.23666349.v1

Gao, C., Zhang, R.-H., Karnauskas, K. B., Zhang, L., & Tian, F. (2020). Separating freshwater flux effects on ENSO in a hybrid coupled model of the tropical Pacific. *Climate Dynamics*, *54*(11), 4605–4626. https://doi.org/10.1007/s00382-020-05245-y

Geng, T., Cai, W., Wu, L., Santoso, A., Wang, G., Jing, Z., et al. (2022). Emergence of changing central-Pacific and eastern-Pacific El Niño-Southern Oscillation in a warming climate. *Nature Communications*, *13*(1), 6616. https://doi.org/10.1038/s41467-022-33930-5

Gent, P. R., & Cane, M. A. (1989). A reduced gravity, primitive equation model of the upper equatorial ocean. *Journal of Computational Physics*, *81*(2), 444–480. https://doi.org/10.1016/0021-9991(89)90216-7

Guan, C., Hu, S., McPhaden, M. J., Wang, F., Gao, S., & Hou, Y. (2019). Dipole structure of mixed layer salinity in response to El Niño-La Niña asymmetry in the tropical pacific. *Geophysical Research Letters*, *46*(21), 12165–12172. https://doi.org/10.1029/2019gl084817

Guan, C., & McPhaden, M. J. (2016). Ocean processes affecting the twenty-first-century shift in ENSO SST variability. *Journal of Climate*, *29*(19), 6861–6879. https://doi.org/10.1175/jcli-d-15-0870.1

Guan, C., McPhaden, M. J., Wang, F., & Hu, S. (2019). Quantifying the role of oceanic feedbacks on ENSO asymmetry. *Geophysical Research Letters*, *46*(4), 2140–2148. https://doi.org/10.1029/2018gl081332

Guan, C., Tian, F., McPhaden, M. J., Wang, F., Hu, S., & Zhang, R.-H. (2022). Zonal structure of tropical Pacific surface salinity anomalies affects ENSO intensity and asymmetry. *Geophysical Research Letters*, *49*(1), e2021GL096197. https://doi.org/10.1029/2021gl096197

Guan, C., Wang, X., & Yang, H. (2023). Understanding the development of the 2018/19 central Pacific El Niño. *Advances in Atmospheric Sciences*, *40*(1), 177–185. https://doi.org/10.1007/s00376-022-1410-1

Huang, B., Thorne, P. W., Banzon, V. F., Boyer, T., Chepurin, G., Lawrimore, J. H., et al. (2017). Extended reconstructed Sea surface temperature, Version 5 (ERSSTv5): Upgrades, validations, and intercomparisons [Dataset]. Journal of Climate, *30*(20), 8179–8205. https://doi.org/10.1175/JCLI-D-16-0836.1

Kalnay, E., Kanamitsu, M., Kistler, R., Collins, W., Deaven, D., Gandin, L., et al. (1996). The NCEP/NCAR 40-year reanalysis project [Dataset]. Bulletin of the American Meteorological Society, *77*(3), 437–471. https://doi.org/10.1175/1520-0477(1996)077<0437:tnyrp>2.0.co;2

Kao, H.-Y., & Yu, J.-Y. (2009). Contrasting eastern-Pacific and central-Pacific types of ENSO. *Journal of Climate*, *22*(3), 615–632. https://doi.org/10.1175/2008jcli2309.1

Kug, J. S., Jin, F.-F., & An, S.-I. (2009). Two types of El Niño events: Cold tongue El Niño and warm pool El Niño. *Journal of Climate*, *22*(6), 1499–1515. https://doi.org/10.1175/2008JCLI2624.1

Larkin, N. K., & Harrison, D. E. (2005a). On the definition of El Niño and associated seasonal average U.S. weather anomalies. *Geophysical Research Letters*, *32*(13), L13705. https://doi.org/10.1029/2005GL022738

Larkin, N. K., & Harrison, D. E. (2005b). Global seasonal temperature and precipitation anomalies during El Niño autumn and winter. *Geophysical Research Letters*, *32*(16), L16705. https://doi.org/10.1029/2005GL022860

Lee, T., & McPhaden, M. J. (2010). Increasing intensity of El Niño in the central-equatorial Pacific. *Geophysical Research Letters*, *37*(14), L14603. https://doi.org/10.1029/2010GL044007

Luo, Y., Rothstein, L. M., Zhang, R.-H., & Busalacchi, A. J. (2005). On the connection between South Pacific subtropical spiciness anomalies and decadal equatorial variability in an ocean general circulation model. *Journal of Geophysical Research*, *110*(C10), C10002. https://doi.org/10.1029/2004jc002655

Maes, C., Ando, K., Delcroix, T., Kessler, W. S., McPhaden, M. J., & Roemmich, D. (2006). Observed correlation of surface salinity, temperature and barrier layer at the eastern edge of the western Pacific warm pool. *Geophysical Research Letters*, *33*(6), L06601. https://doi.org/10.1029/2005gl024772

Maes, C., Picaut, J., & Belamari, S. (2002). Salinity barrier layer and onset of El Nino in a Pacific coupled model. *Geophysical Research Letters*, *29*(24), 5951–5954. https://doi.org/10.1029/2002gl016029

Maes, C., Picaut, J., & Belamari, S. (2005). Importance of the salinity barrier layer for the buildup of El Nino. *Journal of Climate*, *18*(1), 104–118. https://doi.org/10.1175/jcli-3214.1

McPhaden, M. J., Zebiak, S. E., & Glantz, M. H. (2006). ENSO as an integrating concept in Earth science. *Science*, *314*(5806), 1740–1745. https://doi.org/10.1126/science.1132588

Murtugudde, R., & Busalacchi, A. J. (1998). Salinity effects in a tropical ocean model. *Journal of Geophysical Research*, *103*(C2), 3283–3300. https://doi.org/10.1029/97jc02438

Qi, J., Zhang, L., Qu, T., Yin, B., Xu, Z., Yang, D., et al. (2019). Salinity variability in the tropical Pacific during the central-Pacific and eastern-Pacific El Niño events. *Journal of Marine Systems*, *199*, 103225. https://doi.org/10.1016/j.jmarsys.2019.103225

Ren, H., & Jin, F. (2013). Recharge oscillator mechanisms in two types of ENSO. *Journal of Climate*, *26*(17), 6506–6523. https://doi.org/10.1175/JCLI-D-12-00601.1

Schneider, N. (2004). The response of tropical climate to the equatorial emergence of spiciness anomalies. *Journal of Climate*, *17*(5), 1083–1095. https://doi.org/10.1175/1520-0442(2004)017<1083:trotct>2.0.co;2

Singh, A., Delcroix, T., & Cravatte, S. (2011). Contrasting the flavors of El Niño-Southern Oscillation using sea surface salinity observations. *Journal of Geophysical Research*, *116*(C6), C06016. https://doi.org/10.1029/2010jc006862

Sullivan, A., Luo, J.-J., Hirst, A. C., Bi, D., Cai, W., & He, J. (2016). Robust contribution of decadal anomalies to the frequency of central Pacific El Niño. *Scientific Reports*, *6*(1), 38540. https://doi.org/10.1038/srep38540

Timmermann, A., An, S., Kug, J. S., Jin, F. F., Cai, W., Capotondi, A., et al. (2018). El Nino Southern oscillation complexity. *Nature*, *559*(7715), 535–545. https://doi.org/10.1038/s41586-018-0252-6

Vialard, J., & Delecluse, P. (1998a). An OGCM study for the TOGA decade. Part I: Role of salinity in the physics of the western Pacific fresh pool. *Journal of Physical Oceanography*, *28*(6), 1071–1088. https://doi.org/10.1175/1520-0485(1998)028<1071:aosftt>2.0.co;2

Vialard, J., & Delecluse, P. (1998b). An OGCM study for the TOGA decade. Part II: Barrier-layer formation and variability. *Journal of Physical Oceanography*, *28*(6), 1089–1106. https://doi.org/10.1175/1520-0485(1998)028<1089:aosftt>2.0.co;2

Vialard, J., Delecluse, P., & Menkes, C. (2002). A modeling study of salinity variability and its effects in the tropical Pacific Ocean during the 1993–1999 period. *Journal of Geophysical Research*, *107*(C12), 1–14. https://doi.org/10.1029/2000jc000758

Yu, L., & Weller, R. A. (2007). Objectively analyzed Air–Sea heat fluxes for the global ice-free oceans (1981–2005) [Dataset]. *88*(4), 527–540. Bulletin of the American Meteorological Society. https://doi.org/10.1175/BAMS-88-4-527

Zhang, R.-H. (2015). A hybrid coupled model for the Pacific Ocean–atmosphere system. Part I: Description and basic performance. *Advances in Atmospheric Sciences*, *32*(3), 301–318. https://doi.org/10.1007/s00376-014-3266-5

Zhang, R.-H., & Busalacchi, A. J. (2009). Freshwater flux (FWF)-induced oceanic feedback in a hybrid coupled model of the tropical Pacific. *Journal of Climate*, *22*(4), 853–879. https://doi.org/10.1175/2008jcli2543.1

Zhang, R.-H., Tian, F., & Wang, X. (2018). Ocean chlorophyll-induced heating feedbacks on ENSO in a coupled ocean physics-biology model forced by prescribed wind anomalies. *Journal of Climate*, *31*(5), 1811–1832. https://doi.org/10.1175/jcli-d-17-0505.1

Zhang, R.-H., Zheng, F., Zhu, J. S., Pei, Y. H., Zheng, Q. N., & Wang, Z. G. (2012). Modulation of El Nino-southern oscillation by freshwater flux and salinity variability in the tropical Pacific. *Advances in Atmospheric Sciences*, *29*(4), 647–660. https://doi.org/10.1007/s00376-012-1235-4

Zhao, M., Hendon, H. H., Alves, O., & Yin, Y. (2014). Impact of improved assimilation of temperature and salinity for coupled model seasonal forecasts. *Climate Dynamics*, *42*(9–10), 2565–2583. https://doi.org/10.1007/s00382-014-2081-0

Zheng, F., Zhang, R.-H., & Zhu, J. (2014). Effects of interannual salinity variability on the barrier layer in the western-central equatorial Pacific: A diagnostic analysis from Argo. *Advances in Atmospheric Sciences*, *31*(3), 532–542. https://doi.org/10.1007/s00376-013-3061-8

Zhi, H., Zhang, R.-H., Lin, P., Yu, P., Zhou, G., & Shi, S. (2020). Interannual salinity variability associated with the central Pacific and eastern Pacific El Ninos in the Tropical Pacific. *Journal of Geophysical Research: Oceans*, *125*(10), e2020JC016090. https://doi.org/10.1029/2020jc016090

Zhi, H., Lin, P., Fang, Z., Liu, H., Zhang, R. H., & Bai, W. (2021). Sea surface salinity-derived indexes for distinguishing two types of El Nino events in the tropical Pacific. *Science China Earth Sciences*, *64*(8), 18–1284. https://doi.org/10.1007/s11430-020-9780-2

Zuo, H., Balmaseda, M. A., de Boisseson, E., Hirahara, S., Chrust, M., & De Rosnay, P. (2017). A generic ensemble generation scheme for data assimilation and ocean analysis [Dataset]. ECMWF Tech Memo. https://doi.org/10.21957/cub7mq0i4